Electronic Supplementary Material (ESI) for Physical Chemistry Chemical Physics.
This journal is © the Owner Societies 2020

Supplementary Material of "Two-dimensional van der Waals heterostructure CdO/PtSe$_2$: promising visible light photocatalyst for overall water splitting"

Wei Zhang[a,b*], Weixiao Ji[c]

[a)] Physicochemical Group of College of Criminal Science and Technology & Forensic Center of Public Security of Bureau of National Forestry Bureau, Nanjing Forest Police College, Nanjing, 210023, China
[b)] NNU-SULI Thermal Energy Research Center (NSTER) & Center for Quantum Transport and Thermal Energy Science (CQTES), School of Physics and Technology, Nanjing Normal University, Nanjing 210023, China
[c)] Spintronics Institute, School of Physics and Technology, University of Jinan, Jinan 250022, China

*E-mail: zhangw@nfpc.edu.cn
Phone: +86 025 85878792

Outline

Fig. S1: Crystal structures of six patterns of CdO/$PtSe_2$ heterostructure. The Cd, O, Pt and Se atoms are respectively marked by purple, red, grey and green. The dashed lines denote the primitive cell.

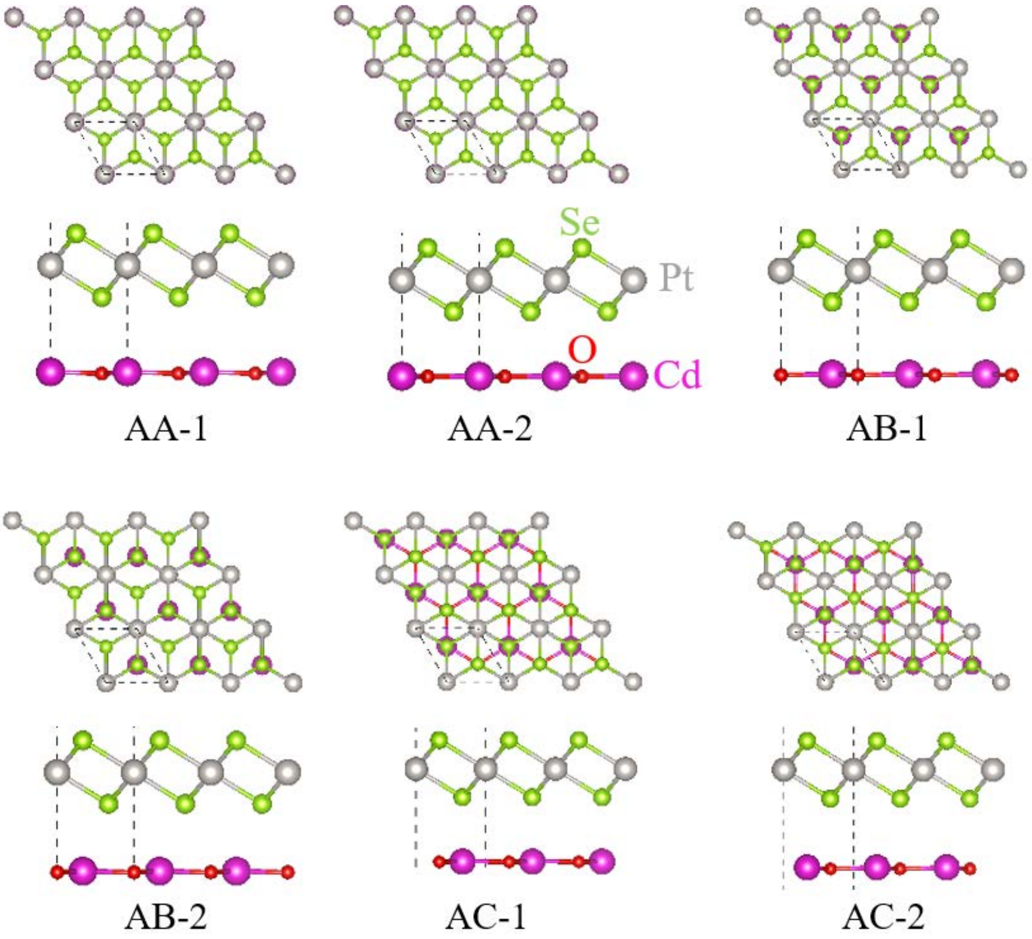

AA-1 AA-2 AB-1

AB-2 AC-1 AC-2

Fig. S2: Layer projected DOS of AA-2 with denser gridpoints. For all the DOS calculations, the tetrahedron method with Blöchl corrections is used. In VASP, the parameter “NEDOS” specifies number of gridpoints on which the DOS is evaluated. In Fig. 2 of main text, the NEDOS=600 is used. To make the layer contributions to the VBM more clear, a denser gridpoints with NEDOS=2000 is used. Take the AA-2 pattern as example, we can clearly see that the VBM is contributed by CdO, which is consistent with the band dispersions and band decomposed charge densities of VBM.

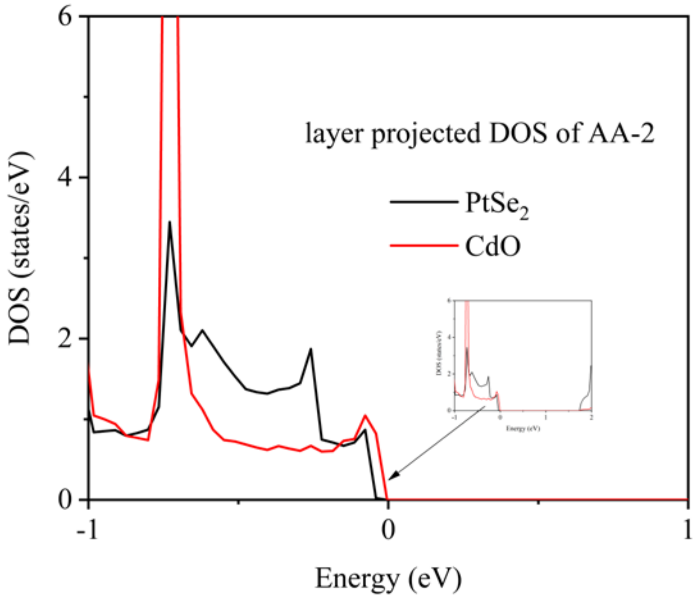

Fig. S3: Layer projected DOS of AA-1, AB-1, AC-1 and AC-2. The DOS of CdO and $PtSe_2$ is respectively marked by red and blue. The blue line denotes the DOS border of $PtSe_2$ covered by CdO. In AA-1, the VBMs of CdO and $PtSe_2$ are degenerated, the CBM is mainly contributed by the $PtSe_2$. Other patterns all have the Type-II band alignments, i.e. the VBM and CBM are respectively contributed by CdO and $PtSe_2$.

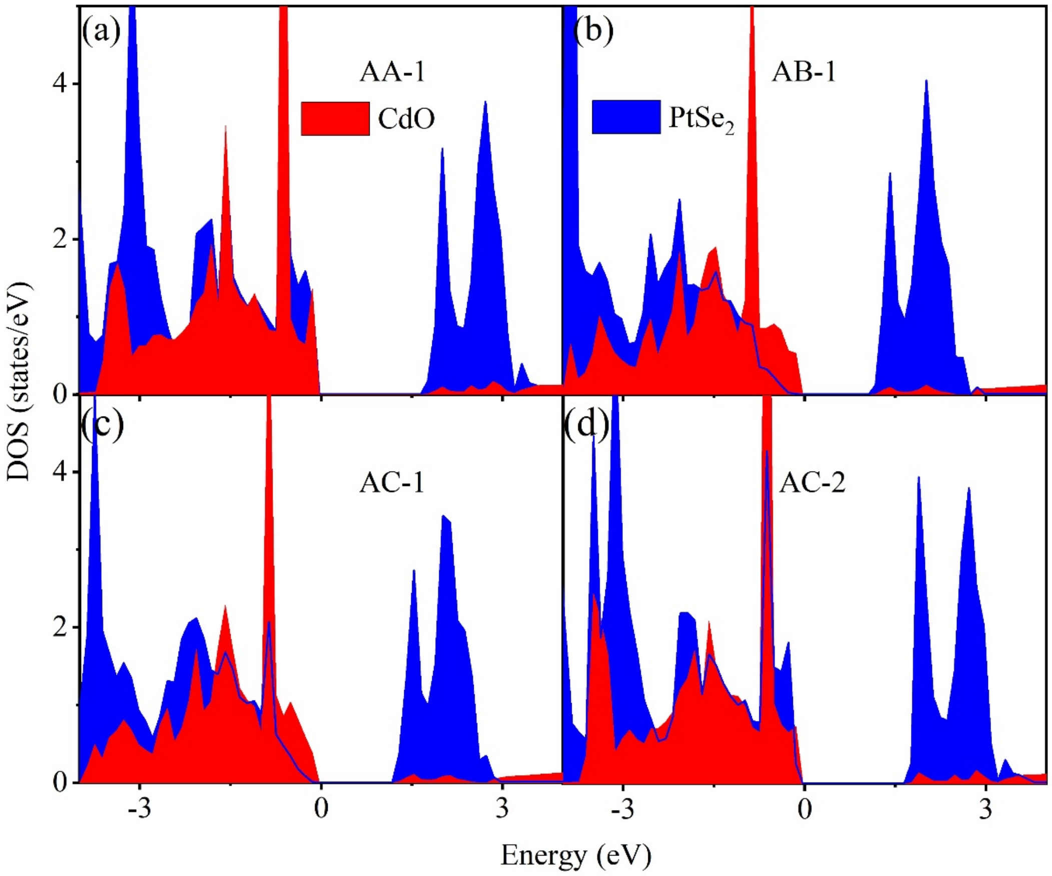

Table S1: The carrier mobility (μ) of CdO/PtSe$_2$ (AA-2) calculated by GGA.

m^*_x	m^*_y	E_{1x}	E_{1y}	$C_{\text{2D-}x}$	$C_{\text{2D-}y}$	μ_x	μ_y
Electrons							
0.28	0.24	1.92	2.55	100.97	100.71	8107.09	5284.19
Holes							
1.1	1.17	1.69	1.79	100.97	100.71	605.76	506.33

The rectangular cell shown below is used to calculate the carrier mobility. The most stable AA-2 pattern is taken as example. The μ (cm^2 V^{-1} s^{-1}) is calculated by $\mu = \frac{e\hbar^3 C_{2D}}{k_B T m^* m_d E_1^2}$ according to the deformation potential theory.

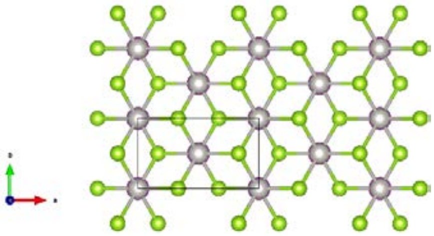

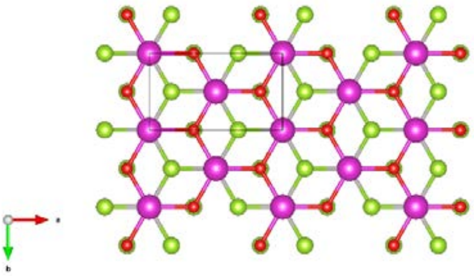

μ_x and μ_y are the carrier mobilities along the armchair and zigzag directions. T=300 K. m^* is the effective mass along the x or y direction, $m_d = \sqrt{m_x m_y}$. E_1 (eV) is deformation potential constant, $E_1 = \Delta E/\varepsilon$, strain $\varepsilon = \Delta l/l_o$, l_o is the equilibrium lattice constant along the x or y direction, ΔE is the change of VBM or CBM induced by the small strain ε(Δl, change of lattice constants). C_{2D} (N m^{-1}) is the in-plane stiffness, $C_{2D} = \frac{\partial^2 E}{\partial \varepsilon^2}$. Previous calculations by LDA (Zhang *et al.*, Nano Res., 2014, 7, 1731) showed that the electron m^* and μ of 1L PtSe$_2$ are respectively 0.19-0.21 (along Γ-K, K-M) and 1892.

We can see that the m^* of electrons (CBM is consisted by PtSe$_2$) is a little heavier than the 1L PtSe$_2$, but they are lighter than the common MX$_2$ (X=S, Se, Te) with the m^* of 0.45-0.57 (Zhang *et al.*, Nano Res., 2014, 7, 1731). The formation of heterostructure increases the electron mobility. Though the electron mobility is smaller than the well-known graphene, it is significantly larger than the common MX$_2$ systems. The m^* of CdO/PtSe$_2$ is lighter than (or comparable with) the 1L C$_3$N$_4$ and C$_3$N$_4$/B$_4$C$_3$ (Mahmood *et al.*, Appl. Catal. B: Environ., 2020, 278, 119310). The heavy m^* of holes (VBM is consisted by CdO) is due to the relatively flat band dispersions around the VBM, the corresponding μ is thus smaller than the electrons, but are larger than the electron mobility of MoX$_2$ (X=S, Se), SnX$_2$ (X=S, Se).

Fig. S4: Carrier density distributions around CBM(VBM). Basing on the GGA calculated effective mass (m_d^* in Table S1) of hole(electron), we plot the carrier density distributions according to the formulas $n_h=2(\frac{m_h^{*}k_BT}{2\pi\hbar^2})^{3/2}e^{\frac{-(E_F-E)}{k_BT}}\ (E\leq E_v)$, $n_e=2(\frac{m_e^{*}k_BT}{2\pi\hbar^2})^{3/2}e^{\frac{-(E-E_F)}{k_BT}}\ (E\geq E_c)$, which can be found in the textbook of solid state physics or e.g. https://en.wikipedia.org/wiki/Charge_carrier_density. The formulas are suitable for semiconductors near room temperature. $m_h(m_e)$ is the hole(electron) effective mass, $E_c(E_v)$ is the energy of CBM(VBM), E_F is the Fermi level, $n_h(n_e)$ is the density of hole(electron), T=300 K.

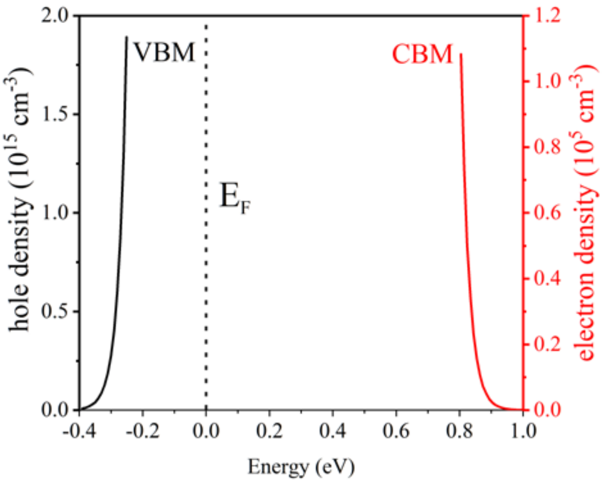

Fig. S5: The enlarged planar-average electrostatic potential along the z axis of AA-2 and AB-2. The Δϕs of AA-2 and AB-2 are relatively smaller than other patterns, different scales are used here.

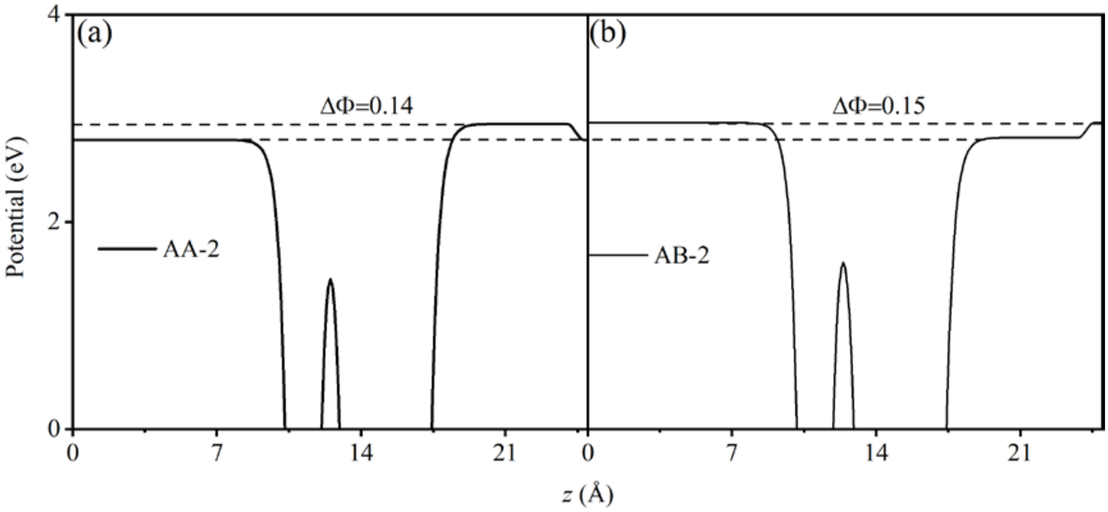

Fig. S6: Planar-average electrostatic potential along the *z* axis of AA-1, AB-1, AC-1 and AC-2.

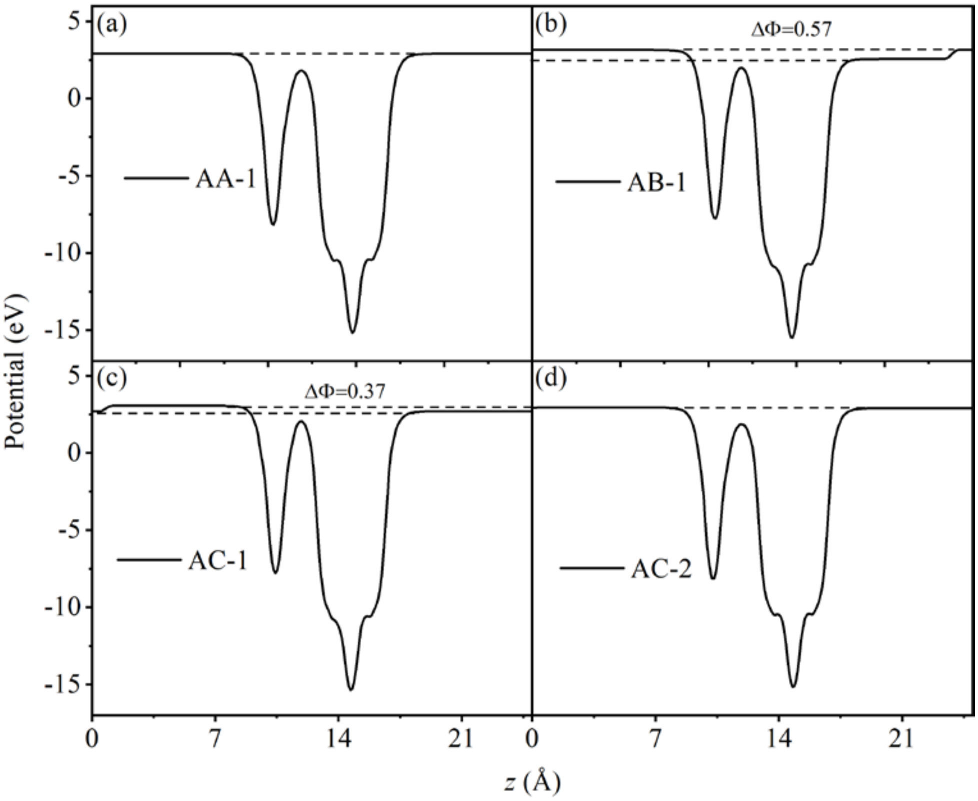

Fig. S7: Band alignment of AB-1. The water redox levels on the CdO and $PtSe_2$ sides are respectively marked by red and blue. AB-1 has a band gap (1.21 eV) less than 1.23 eV. We can see below that it still straddle the water redox levels.

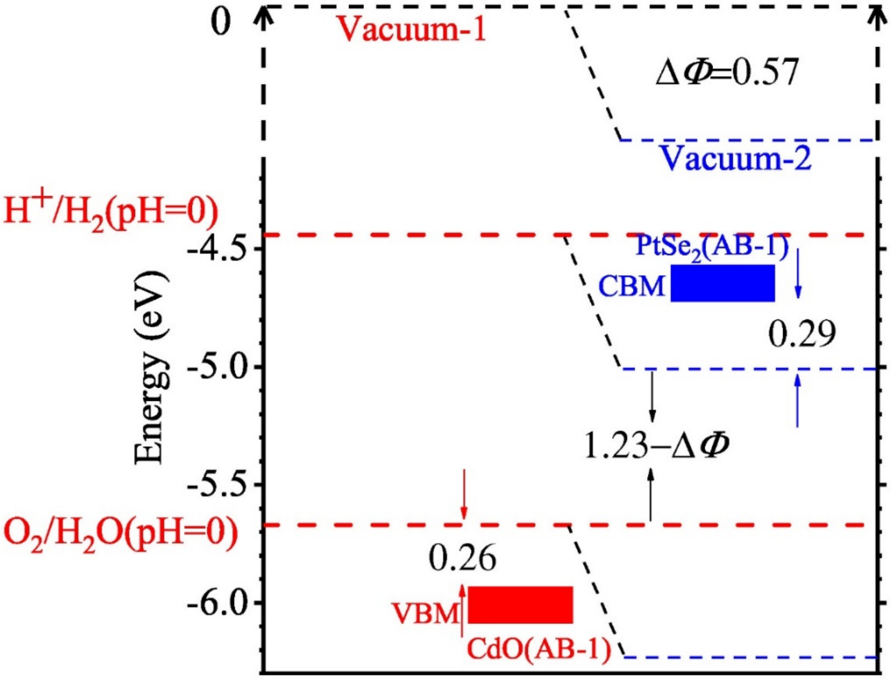

Fig. S8: Band alignment with respect to the normal hydrogen electrode (NHE). Take the case of 1L CdO and 1L $PtSe_2$ as examples. In the main text, the vacuum level is taken as reference. The experimentalists use the NHE as reference. Their relation is shown below. The dashed lines denote the standard redox potentials of water at pH=0.